BMB Reports - Manuscript Submission

Manuscript Draft

Manuscript Number: BMB-20-228

Title: Diffusion-based determination of protein homodimerization on reconstituted membrane surfaces

Article Type: Mini Review

Keywords: In vitro membrane reconstitution; dimerization; fluorescence correlation spectroscopy; single molecule tracking

Corresponding Author: Jean Chung

Authors: Tyler Jepson[1], Jean Chung[1,*]

Institution: [1]Chemistry, Colorado State University,

Manuscript type: Mini Review

Title: Diffusion-based determination of protein homodimerization on reconstituted membrane surfaces

Authors: Tyler A. Jepson, Jean K. Chung

Affiliation: Department of Chemistry, Colorado State University, Fort Collins, CO 80523 USA

Running title: Measurement of membrane dimerization by diffusion

Keywords: *In vitro* membrane reconstitution, dimerization, fluorescence correlation spectroscopy, single molecule tracking

Corresponding author's information: Phone: (970) 491-6842 e-mail: jkchung@colostate.edu

Abstract

The transient interactions between cellular components, particularly on membrane surfaces, are critical in the proper function of many biochemical reactions. For example, many signaling pathways involve dimerization, oligomerization, or other types of clustering of signaling proteins as a key step in the signaling cascade. However, it is often experimentally challenging to directly observe and characterize the molecular mechanisms such interactions—the greatest difficulty lies in the fact that living cells have an unknown number of background processes that may or may not participate in the molecular process of interest, and as a consequence, it is usually impossible to definitively correlate an observation to a well-defined cellular mechanism. One of the experimental methods that can quantitatively capture these interactions is through membrane reconstitution, whereby a lipid bilayer is fabricated to mimic the membrane environment, and the biological components of interest are systematically introduced, without unknown background processes. This configuration allows the extensive use of fluorescence techniques, particularly fluorescence fluctuation spectroscopy and single-molecule fluorescence microscopy. In this review, we describe how the equilibrium diffusion of two proteins, K-Ras4B and the PH domain of Bruton's tyrosine kinase (Btk), on fluid lipid membranes can be used to determine the kinetics of homodimerization reactions.

Introduction

The cellular membrane is the primary theater of signal transduction, which begins at the receptor binding at the membrane surface and the subsequent downstream (1, 2). Transient protein-protein and protein-lipid interactions on membrane surfaces constitute the key steps in these signaling cascade reactions (2-5). These interactions are often combinatorial in design, involving reactions such as homo- and hetero-oligomerization (6-10). However, the molecular details of many such systems still remain mysterious. This is largely because mechanistic investigations, which must constitute quantitative measurements, on self-assembled lipid bilayer structures can be a prodigious technical challenge. On experimental systems utilizing live cells, there are added complications due to the copious number of additional background processes which may or may not participate the process under observation. Fortunately, many advances in membrane reconstitution as well as imaging and spectroscopic techniques have made it possible to probe quantitative information such as kinetic rate constants of membrane association and dissociation, catalytic rates, and diffusion constants (16, 19-21). In particular, supported lipid bilayers (SLBs) stand out in its straightforwardness in preparation, experimental implementations, and data analysis (22-28). SLBs are planar lipid bilayers that can be as large as square centimeters in area. They are typically prepared by the rupturing small unilamellar vesicles, which then fuse with each other into a single bilayer on a solid support such as glass coverslips (23, 29).

One way to detect protein-protein interactions on membrane surfaces is by measuring diffusion, which is sensitive to the size of the proteins as well as their conformations, orientations, and overall interaction with the membrane. In addition to the obvious advantages of

SLBs in allowing precise control over their chemical environment, another important advantage is that the SLB lipids and other molecules embedded within are fluid and exhibit unencumbered Brownian diffusion (24, 30, 31). This is in stark contrast with the membrane diffusion in live cells where diffusion is usually anomalous (31). The well-defined diffusion behavior allows the diffusion measurements performed on SLBs to be interpreted without much ambiguity. Thus, SLBs have been demonstrated in its usefulness in many works examining molecular interactions on membrane surfaces. Two such examples are K-Ras4B GTPase (32) and the pleckstrin homology (PH) domain of Bruton's tyrosine kinase (Btk) in their dimerization behavior (33). Homodimerization is perhaps the simplest possible protein-protein interaction and is ubiquitous in signal transduction. Nevertheless, the accurate determination of its kinetics is still a significant technical challenge, particularly if it is dependent on membranes. This is the case for both K-Ras4B and Btk, whose dimerization has never been observed in solution even though they were thought to be critical in their function. In this review, the diffusion-based investigation of their dimerization behavior of K-Ras4B and Btk using fluorescence spectroscopy and imaging will be described.

Two-dimensional diffusion on membranes

While it can be reasonably assumed that the diffusion coefficient of a molecule tethered to a membrane would be dependent on its overall size, their theoretical relationship is not necessarily straightforward. In a three-dimensional space, particle diffusion follows Stokes-Einstein relation, where the diffusion coefficient D is inversely proportional to the hydrodynamic radius r of the particle (**Equation 1**),

$$D = \frac{k_B T}{f} = \frac{k_B T}{6\pi\eta r}$$

Where k_B is Boltzmann's constant, T is the absolute temperature, f is the friction, and η is the viscosity of the medium. In so-called Stokes' Paradox, however, no simple relationship between the particle size and the diffusion coefficient in two dimensions. In specific case of a cylinder embedded in a viscous two-dimensional medium (such as a lipid bilayer), its diffusion is described by Saffman-Delbruck model, in which diffusion coefficient is proportional to the natural log of inverse radius of the cylinder (34). Experiments have mixed results with respect to this model's ability to accurately predict the diffusion from the protein size (35, 36). Nevertheless, the model's assumptions are incompatible with many membrane proteins if they deviate from the cylindrical shape with heights mismatching that of the membrane. Thus, the applicability of Saffman-Delbruck model is limited in cases such as peripheral membrane proteins that are only associated with one leaflet of the membrane to varying degrees.

For peripheral membrane proteins, many factors influence the observed diffusion: (1) the number of lipid anchors attached to the protein, if any, (2) the degree of immersion and interaction (including nonspecific ones such as Coulomb interactions) of the protein with the membrane, (3) the structure and orientation of the protein with respect to the membrane, among others (37). Without a detailed knowledge of these factors, it is in principle impossible to predict the diffusion behavior of the peripheral membrane proteins. A useful alternative is to experimentally calibrate the diffusion coefficients as a function of the molecular size of the proteins. In an in vitro study by Knight et al (38), multimers of pleckstrin homology (PH) domains of general receptor of phosphoinositides 1 (Grp1), which selectively binds to

phosphatidylinositol (3,4,5)-trisphosphate (PIP_3) lipids were engineered, and their diffusion on supported lipid bilayers were measured as a function of the lipid binding stoichiometry. It was found that diffusion coefficient is inversely proportional to the number of lipid anchors–in other words, the PH multimers followed Stokes-Einstein relation (**Equation 2**):

$$D = k_B T/(f_1 + f_2 + \cdots + f_N)$$

Where f_N is the additive friction introduced by the Nth lipid anchor.

Diffusion measurements by fluorescence

Fluorescence spectroscopy and microscopy are by far the most common methods to measure diffusion on biological membranes. Among various techniques, fluorescence correlation spectroscopy (FCS) and single-molecule tracking (SMT) with surface-selective total internal reflection microscopy (TIRFM) offer high precision and reliability and have been used in a number of studies seeking to establish molecular interactions (Figure 1), including the K-Ras4B and Btk PH domain studies.

Fluorescence correlation spectroscopy. FCS is a type of fluorescence fluctuation spectroscopy (FFS), which are techniques based on the time-dependent fluorescence intensity fluctuations. It was invented in more than thirty years ago (39), but it has not been very useful until the widespread use of very stable lasers in more recent years. FCS is now commonly used to characterize biological molecules in solutions, membranes, and in live cells (40, 41). It relies on observing fluorescent molecules in a laser focus, which is typically close to diffraction-

limited and very small focus volume (~ 10^{-15} L). Therefore, the number of molecules observed is very small—which is why sometimes they are considered "single-molecule" techniques (42). The time-dependent intensity fluctuations are due to fluorescent molecules diffusing in and out of the focus, and therefore contain information about the average number of the molecules within the focus volume and their diffusivity (Figure 1A). To extract these information, the autocorrelation function ACF of the fluorescence intensity fluctuation trace is computed, and it is fit to a autocorrelation model with Gaussian focus G(τ). For a two-dimensional Brownian diffusion, the model is given by (**Equation 3**)

$$G(\tau) = \frac{1}{N}\left(1 + \frac{4D\tau}{w^2}\right)^{-1}$$

Where N is the number of the particles in the focus, D is the diffusion coefficient, τ is the average focus residence time of the molecule, and w is the radius of the Gaussian focus. Therefore, the absolute values of concentration and diffusion coefficient may be obtained with calibrated focus radius w.

An added benefit in using FCS to detect multimerization of fluorescent molecules is that it is particularly sensitive to brighter species. If there are mixed species present in FCS, the autocorrelation model is given by **(Equation 4)**

$$G(\tau) = \frac{\sum N_i B_i^2 D_i(\tau)}{(\sum N_i B_i)^2}$$

Where B_i is the molecular brightness of the *i*th species and $D(\tau) = \left(1 + \frac{4D\tau}{w^2}\right)^{-1}$ (32). Note that the overall autocorrelation is dependent on the *square* of B_i, so brighter species will contribute nonlinearly to the overall autocorrelation, and further outweighs the contribution by *N*. For example, if the sample is an equimolar mixture of a monomer with brightness with *B* and dimer of brightness 2*B*, the detected autocorrelation will be mostly due to the dimer even though the concentrations of monomers and dimers are the same. This "exaggerated" presence of brighter species is particularly advantageous in detecting and measuring the multimeric species where the multimerization affinities are very weak and there is only a small fraction of dimers in a mostly monomeric system.

Single-molecule tracking. In SMT, the motions of single fluorophores are directly visualized and captured by a high quantum efficiency camera (4, 17, 30, 37, 43, 44). By using extrinsic fluorophores of high quantum yield and photostability, long-lived, high signal-to-noise ratio trajectories of single molecules can be recorded (Figure 1B). In the data analysis, the molecule position is identified, and by linking them the particles between teach time frame, a trajectory for each molecule is constructed (45). Thousands of such trajectories can be collected in a single movie, and the diffusion coefficient *D* of the particles can be obtained by analyzing the step size distribution $P(r)$ given by **(Equation 5)**

$$P(r, t; D) = \frac{r}{2Dt} \exp\left(-\frac{r^2}{4Dt}\right)$$

Where r is the particle displacement and t is the time interval (16, 30, 46). If there are two distinct diffusing populations with diffusion coefficients D_1 and D_2, the distribution is **(Equation 6)**

$$P(r,t;D_1,D_2,\alpha) = \frac{\alpha r}{2D_1 t}\exp\left(-\frac{r^2}{4D_1 t}\right) + \frac{(1-\alpha)r}{2D_2 t}\exp\left(-\frac{r^2}{4D_2 t}\right)$$

Where α is the relative population of the diffusing species with diffusion coefficient D_1. Thus, provided that the camera has a sufficient frame rate to resolve the step sizes associated with diffusion coefficients for monomeric and dimeric species, SMT is capable of resolving the diffusion coefficients and relative populations of monomers and dimers. A practical consideration in the implementation of SMT experiments the surface density of fluorophores must be kept low as to spatially resolve the diffusing species. Stoichiometric under-labeling of fluorophores (for example, if one in 10^6-10^9 molecules are labeled with a fluorophore on a bilayer with a surface density of 1,000 molecules/μm^2, there are <100 fluorescent molecules per field of view in a typical EMCCD camera) is frequently used to achieve this condition (17, 47).

Dimerization of Ras

K-Ras4B is one of four isoforms of Ras, which is a central molecular switch in a number of signaling pathways such as the mitogen-activated protein kinase (MAPK) and phosphoinositide 3-kinases (PI3K)-AKT pathways (13, 14). A small globular protein that is tethered to the membrane by a lipid anchor, Ras—and especially K-Ras4B—is of a paramount clinical importance in that its oncogenic mutations, where it is unable to return to the GDP-

bound "off" state, are found in ~30% of all human cancers (48). Despite concerted efforts to develop therapeutic strategies to inhibit Ras, all conventional, small molecule-based competitive inhibitors to date have failed (49). This has led to an interest in novel strategies to target Ras by modulating its spatial organization, as Ras is observed in dimers and clusters on cellular surfaces (50-53). In particular, it was speculated that its dimerization drove the assembly—this was supported by the consistent dimeric structures in crystals, as well as the fact that some interacting partners of Ras do so in pairs (for example, SOS interacts with two Ras molecules, as described) (54-56). However, Ras dimers are never observed in solution, and despite many attempts to detect them on membranes no consensus exists regarding the nature of Ras dimers—whether they are intrinsic properties of Ras, or if so, which specific interactions are responsible—and even whether they exist at all (47, 57-60).

Whether natively expressed and fully processed K-Ras4B can homodimerize on its own on membrane surfaces without extrinsic factors was investigated by using SLB-based reconstitution, FCS, and SMT (32, 61). Two fluorescent labeling strategies were used: eGFP fused to K-Ras4B and an extrinsically labeled guanosine nucleotides that binds to K-Ras4B, and both displayed identical results. A definitive answer to this question would involve a measurement of the two-dimensional dissociation constant, K_d^{2d}, of the dimerization reaction,

(Equation 7)

$$Ras + Ras \rightleftharpoons Ras_2 \quad \text{with} \quad K_d^{2d} = \frac{\sigma_{Ras_2}^2}{\sigma_{Ras}}$$

Where σ_{Ras}^2 and $\sigma_{Ras_2}^2$ are equilibrium surface densities of Ras monomers and dimers, respectively. The basic strategy to determine the dissociation constant was to measure the change in diffusion, induced by dimerization, as a function of surface density: in other words, obtain a titration curve where the readout for the surface density of dimers was the decrease in average

diffusion. The theoretical surface density titration is shown in Fig. 1C, left panel. A number of titration curves for a range of K_d are plotted; a dimerization reaction with K_d of 200 molecules/μm^2 indicates a fairly strong dimerization affinity, whereas K_d of 1.25 x 10^4 molecules/μm^2 would represent a dimerization affinity so weak that it is only significant at a protein surface density approaching the close-packed state.

This strategy requires the knowledge of protein surface density and the diffusion coefficients of the monomers and dimers. While the surface density and diffusion coefficient of monomers may be readily measured by FCS or SMT, it is less straightforward to measure the diffusion coefficient of dimers of unknown dissociation constant, especially if it is weak. This problem was addressed by deliberately inducing dimerization using a strong cross-linker, in this case the Ras binding domain (RBD) of c-Raf fused to leucine zipper (LeuZ) motif (RBD-LeuZ). RBD selectively binds to GTP-bound Ras, and LeuZ is a constitutively dimeric motive. Therefore, the introduction of LeuZ to GTP-bound Ras results in crosslinking of Ras via LeuZ, and the diffusion coefficient of the dimeric Ras could be determined. In this case, the diffusion coefficient a dimer was approximately half that of a monomer, akin to the system constructed by PH domain multimers (38).

Because it was expected that Ras would have a very weak dimerization affinity, it was important to establish the detection limit of the measurement. Using the experimentally determined values of the diffusion coefficients of monomers and dimers, theoretical FCS titration measurements for a range of dissociation constants were simulated (Figure 1C, right). The simulation shows that, due to the nonlinear contribution of brighter species to the overall measurement, FCS provides a wide dynamic range from strong to very weak dimerization reactions. The brightness effect is so prominent that even dimerization reactions so weak that its

K_d is in the surface density range of close-packed proteins would be detected by FCS within the experimentally accessible surface density (~1,500 molecules/μm^2).

The diffusion measurements indicated that by itself, K-Ras4B remained unambiguously monomeric. Figure 2A shows representative FCS and SMT step-size distribution data. In FCS (Figure 2A, left), GTP-bound K-Ras4B does not change significantly with respect to increasing surface density, unlike K-Ras4B crosslinked by RBD-LeuZ. The estimated K_d for GTP-bound K-Ras was 1.25 x 10^5 μm^2, which is close to the close-packed density (62) for the protein—indicating effectively no dimerization. The same was observed with SMT step size distributions: they are independent of the overall surface density, unless there is the crosslinker present (Figure 2A, right). The same was observed in all conditions tested, such as different membrane lipid compositions including cholesterol, activation states, and chemical environments. These results suggested that higher order multimerization of Ras observed on cells are not driven by its intrinsic dimerization capability, but rather by other factors, such as scaffolding factors or downstream proteins, may be involved.

Dimerization of Bruton's tyrosine kinase (Btk) Pleckstrin homology (PH) domain

Bruton's tyrosine kinase (Btk) is a protein kinase that is critical in activation of B-cells (63, 64). Conventionally, its activation depends on the recruitment to the plasma membrane by interaction with phosphatidylinositol (3,4,5)-trisphosphate (PIP_3) lipids, which are produced upon receptor stimulation. The pleckstrin homology domain fused with a tec homology domain (PH-TH) of Btk selectively binds two PIP_3 headgroups, and results in activation of Btk (65-68). Crystal structures show a consistent dimer structures of the PH-TH domain, and evidence

suggested that *trans*-autophosphorylation (a Btk molecule phosphorylates the other in a dimer) mediated by dimerization may be involved in activation of Btk (69, 70). However, as it was the case for Ras, PH-TH domain dimers were never observed in solution. This led to a speculation that the interaction with the lipid ligand, PIP_3, in the membrane may be required to conformational changes that allow dimerization.

The membrane-dependent dimerization was studied with FCS on supported lipid bilayers. The eGFP-fused PH-TH domain of Btk (an alternative, cysteine-labeled Alexa Fluor 647 also resulted in identical behavior) was introduced to SLBs containing a trace amount (0.005%) of fluorescently labeled lipids (Texas Red-DHPE) and 1-4% PIP_3, and which recruited the protein to the membrane. The diffusion of both eGFP-Btk PH-TH domain and Texas Red-DHPE were simultaneously measured by two-color FCS. The titration curve was obtained by plotting the relative diffusion (PH-TH diffusion divided by lipid diffusion) as a function of the protein surface density. This had an effect of correcting for variations in the measured diffusion arising from microscopic heterogeneity in the membrane environment.

The left panel of Figure 2B shows the FCS titration measurements for the wild type Btk PH-TH domain. There is a robust decrease in the overall diffusion as the surface density is increased on a 4% PIP_3 membrane, consistent with dimerization. It was also found that when the PIP_3 density lower at 1%, there is a substantially less change in diffusion, indicating smaller fraction of dimers at the same protein surface density. To confirm that this observed change in diffusion is due to dimerization, the same experiment was performed with a mutant construct whose putative dimerization interactions (69) had been removed. The resulting titration curve (Figure 2B, right panel) shows that the diffusion is no longer modulated by the increased surface density, indicating that dimerization predicted by the crystal structure is responsible for the

observed changes in diffusion. This observation, combined with adsorption kinetics measurements by total internal fluorescence microscopy, led to a Btk activation model in which each Btk PH-TH domain interacts with two PIP_3 lipids then dimerizes and activates through *trans*-autophosphorylation. It was also suggested that such an elegant combinatorial design in protein-protein and protein-lipid interactions may grant switch-like PIP_3 sensitivity to the Btk activation scheme, which is a common theme in cellular signal transduction (6, 71-73).

Conclusions

Dimerization and higher order multimerization of membrane proteins are a recurring motif in the cellular signal transduction, and a possible protein-protein interaction target for therapeutic interventions. However, it has been challenging to observe complexes and assemblies with traditional *in vitro* strategies, as they fall apart when as soon as membranes are solubilized. They are better preserved and observed on cells, but the platform suffers a different problem that it is difficult to systematically quantify molecular interactions on living cells. Reconstitution strategies such as those using supported lipid bilayers have had shown a great promise, particularly when combined with quantitative fluorescence microscopy such as FCS and SMT. Using diffusion as a readout for molecular interactions allow robust and precise measurement of the dissociation constant. In the case of K-Ras, it was unambiguously shown that it lacks intrinsic ability to dimerize on membranes, suggesting that the clusters observed on cells are assembled by other extrinsic factors. For Btk PH-TH domain, dimerization was never observed in solution even though it was suspected that it was critical in its activation. Its diffusion measurements revealed that the dimerization contact predicted by the crystal structures are responsible for membrane-mediated dimerization. Combined with membrane adsorption

measurements, the entirety of the protein's interaction kinetics were elucidated. While there are limitations to this method in that it can only be applied to reconstituted systems in homogeneous lipid bilayers, these results demonstrate that diffusion-based investigation is a promising strategy for the mechanistic characterization of molecular interactions on membranes. With the continuing advances in microscopy, data analysis algorithms, and membrane fabrication technology, the utility of this method may be expanded to live cell contexts and transmembrane receptors, opening an opportunity to unprecedented understanding the cellular signaling phenomena.

Conflict of Interest

The authors delcare no conflict of interest.

Figure Legends

Figure 1. (A) In fluorescence correlation spectroscopy, a confocal laser illumination spot is used to monitor the intensity fluctuation due to fluorescence molecules diffusing in and out of the focus. The autocorrelation function (ACF) of the resulting time trace is used to compute the particle number (N, from the y-intercept) and residence time (τ_d, from the half-point of the ACF decay) of the fluorescent molecule in the laser focus, which is related to the diffusion coefficient by $w^2 = 4D\tau_d$. In this example, a GFP-labeled protein on a supported lipid bilayer is excited by a blue (488 nm) laser. **(B)** In total internal relfection fluorescence microscopy (TIRFM) single molecule tracking, the displacement of the particle between each frame are reconstructed into particle trajectories (example trajectory shown in inset). The step size distribution may be used to calculate the diffusion coefficient and the relative population of multiple diffusing species, following the step size equation $P(r)$ (Equations 5 and 6 for single and two species, respectively). The fit to a single species step size distribution is shown. **(C)** Left: theoretical binding curves for a dimerization reaction for a wide range of dissociation constants, right: simulated FCS data using experimentally determined diffusion coefficients for monomers and dimers for the same dissociation constants.

Figure 2. (A) Left: FCS data for the dimerization of GTP-bound K-Ras4B (GTP) and GTP-bound K-Ras4B with the RBD-LeuZ crosslinker (GTP + crosslinker) on supported lipid bilayers,

and the estimated dissociation constants for each. The lack of change in diffusion as a function of surface density without the crosslinker suggests that K-Ras4B does not dimerize on its own. Right: step size distributions of K-Ras4B shows similar results: without the crosslinker, there is no change in diffusion as the surface density is increased. **(B)** FCS measurements for the wild type Btk PH-TH domains (left) and the mutant lacking key dimerization residues (right). Substantial dimerization is only observed for the wild type at a high PIP_3 surface density.

References

1. K. M. Eyster, The membrane and lipids as integral participants in signal transduction: lipid signal transduction for the non-lipid biochemist. *Adv Physiol Educ* **31**, 5-16 (2007).
2. J. T. Groves, J. Kuriyan, Molecular mechanisms in signal transduction at the membrane. *Nat Struct Mol Biol* **17**, 659-665 (2010).
3. W. Cho, R. V. Stahelin, Membrane-protein interactions in cell signaling and membrane trafficking. *Annu Rev Biophys Biomol Struct* **34**, 119-151 (2005).
4. R. S. Kasai, S. V. Ito, R. M. Awane, T. K. Fujiwara, A. Kusumi, The Class-A GPCR Dopamine D2 Receptor Forms Transient Dimers Stabilized by Agonists: Detection by Single-Molecule Tracking. *Cell Biochem Biophys* **76**, 29-37 (2018).
5. D. M. Freed *et al.*, EGFR Ligands Differentially Stabilize Receptor Dimers to Specify Signaling Kinetics. *Cell* **171**, 683-695.e618 (2017).
6. K. E. Prehoda, J. A. Scott, R. D. Mullins, W. A. Lim, Integration of multiple signals through cooperative regulation of the N-WASP-Arp2/3 complex. *Science* **290**, 801-806 (2000).
7. J. D. Scott, T. Pawson, Cell signaling in space and time: where proteins come together and when they're apart. *Science* **326**, 1220-1224 (2009).
8. T. Hunter, Tyrosine phosphorylation: thirty years and counting. *Curr Opin Cell Biol* **21**, 140-146 (2009).
9. M. A. Lemmon, Membrane recognition by phospholipid-binding domains. *Nat Rev Mol Cell Biol* **9**, 99-111 (2008).
10. A. C. Newton, Protein kinase C: poised to signal. *Am J Physiol Endocrinol Metab* **298**, E395-402 (2010).
11. S. M. Margarit *et al.*, Structural evidence for feedback activation by Ras.GTP of the Ras-specific nucleotide exchange factor SOS. *Cell* **112**, 685-695 (2003).
12. S. Boykevisch *et al.*, Regulation of ras signaling dynamics by Sos-mediated positive feedback. *Curr Biol* **16**, 2173-2179 (2006).
13. D. K. Simanshu, D. V. Nissley, F. McCormick, RAS Proteins and Their Regulators in Human Disease. *Cell* **170**, 17-33 (2017).
14. F. McCormick, KRAS as a Therapeutic Target. *Clin Cancer Res* **21**, 1797-1801 (2015).
15. J. Gureasko *et al.*, Membrane-dependent signal integration by the Ras activator Son of sevenless. *Nat Struct Mol Biol* **15**, 452-461 (2008).
16. L. Iversen *et al.*, Molecular kinetics. Ras activation by SOS: allosteric regulation by altered fluctuation dynamics. *Science* **345**, 50-54 (2014).
17. Y. K. Lee *et al.*, Mechanism of SOS PR-domain autoinhibition revealed by single-molecule assays on native protein from lysate. *Nat Commun* **8**, 15061 (2017).
18. W. Y. C. Huang *et al.*, A molecular assembly phase transition and kinetic proofreading modulate Ras activation by SOS. *Science* **363**, 1098-1103 (2019).
19. M. D. Vahey, D. A. Fletcher, The biology of boundary conditions: cellular reconstitution in one, two, and three dimensions. *Curr Opin Cell Biol* **26**, 60-68 (2014).
20. Y. H. Chan, S. G. Boxer, Model membrane systems and their applications. *Curr Opin Chem Biol* **11**, 581-587 (2007).
21. M. Chung, R. D. Lowe, Y. H. Chan, P. V. Ganesan, S. G. Boxer, DNA-tethered membranes formed by giant vesicle rupture. *J Struct Biol* **168**, 190-199 (2009).

22. J. T. Groves, M. L. Dustin, Supported planar bilayers in studies on immune cell adhesion and communication. *J Immunol Methods* **278**, 19-32 (2003).
23. W. C. Lin, C. H. Yu, S. Triffo, J. T. Groves, Supported membrane formation, characterization, functionalization, and patterning for application in biological science and technology. *Curr Protoc Chem Biol* **2**, 235-269 (2010).
24. Y. Kaizuka, J. T. Groves, Hydrodynamic damping of membrane thermal fluctuations near surfaces imaged by fluorescence interference microscopy. *Phys Rev Lett* **96**, 118101 (2006).
25. T. C. Buckles, B. P. Ziemba, G. R. Masson, R. L. Williams, J. J. Falke, Single-Molecule Study Reveals How Receptor and Ras Synergistically Activate PI3Kα and PIP. *Biophys J* **113**, 2396-2405 (2017).
26. B. P. Ziemba, J. E. Burke, G. Masson, R. L. Williams, J. J. Falke, Regulation of PI3K by PKC and MARCKS: Single-Molecule Analysis of a Reconstituted Signaling Pathway. *Biophys J* **110**, 1811-1825 (2016).
27. B. P. Ziemba, J. J. Falke, A PKC-MARCKS-PI3K regulatory module links Ca2+ and PIP3 signals at the leading edge of polarized macrophages. *PLoS One* **13**, e0196678 (2018).
28. L. B. Case, J. A. Ditlev, M. K. Rosen, Regulation of Transmembrane Signaling by Phase Separation. *Annu Rev Biophys* **48**, 465-494 (2019).
29. E. Kalb, S. Frey, L. K. Tamm, Formation of supported planar bilayers by fusion of vesicles to supported phospholipid monolayers. *Biochim Biophys Acta* **1103**, 307-316 (1992).
30. B. P. Ziemba, J. J. Falke, Lateral diffusion of peripheral membrane proteins on supported lipid bilayers is controlled by the additive frictional drags of (1) bound lipids and (2) protein domains penetrating into the bilayer hydrocarbon core. *Chem Phys Lipids* **172-173**, 67-77 (2013).
31. J. Humpolícková *et al.*, Probing diffusion laws within cellular membranes by Z-scan fluorescence correlation spectroscopy. *Biophys J* **91**, L23-25 (2006).
32. J. K. Chung *et al.*, K-Ras4B Remains Monomeric on Membranes over a Wide Range of Surface Densities and Lipid Compositions. *Biophys J* **114**, 137-145 (2018).
33. J. K. Chung *et al.*, Switch-like activation of Bruton's tyrosine kinase by membrane-mediated dimerization. *Proc Natl Acad Sci U S A* **116**, 10798-10803 (2019).
34. P. G. Saffman, M. Delbrück, Brownian motion in biological membranes. *Proc Natl Acad Sci U S A* **72**, 3111-3113 (1975).
35. Y. Gambin *et al.*, Lateral mobility of proteins in liquid membranes revisited. *Proc Natl Acad Sci U S A* **103**, 2098-2102 (2006).
36. Y. A. Domanov *et al.*, Mobility in geometrically confined membranes. *Proc Natl Acad Sci U S A* **108**, 12605-12610 (2011).
37. W. C. Lin *et al.*, H-Ras forms dimers on membrane surfaces via a protein-protein interface. *Proc Natl Acad Sci U S A* **111**, 2996-3001 (2014).
38. J. D. Knight, M. G. Lerner, J. G. Marcano-Velázquez, R. W. Pastor, J. J. Falke, Single molecule diffusion of membrane-bound proteins: window into lipid contacts and bilayer dynamics. *Biophys J* **99**, 2879-2887 (2010).
39. D. Magde, E. L. Elson, W. W. Webb, Fluorescence correlation spectroscopy. II. An experimental realization. *Biopolymers* **13**, 29-61 (1974).

40. S. A. Kim, K. G. Heinze, P. Schwille, Fluorescence correlation spectroscopy in living cells. *Nat Methods* **4**, 963-973 (2007).
41. J. Ries, P. Schwille, Fluorescence correlation spectroscopy. *Bioessays* **34**, 361-368 (2012).
42. P. Schwille, S. Kummer, A. A. Heikal, W. E. Moerner, W. W. Webb, Fluorescence correlation spectroscopy reveals fast optical excitation-driven intramolecular dynamics of yellow fluorescent proteins. *Proc Natl Acad Sci U S A* **97**, 151-156 (2000).
43. M. J. Saxton, K. Jacobson, Single-particle tracking: applications to membrane dynamics. *Annu Rev Biophys Biomol Struct* **26**, 373-399 (1997).
44. M. J. Saxton, Single-particle tracking: the distribution of diffusion coefficients. *Biophys J* **72**, 1744-1753 (1997).
45. J. Y. Tinevez *et al.*, TrackMate: An open and extensible platform for single-particle tracking. *Methods* **115**, 80-90 (2017).
46. W. Y. C. Huang, H. K. Chiang, J. T. Groves, Dynamic Scaling Analysis of Molecular Motion within the LAT:Grb2:SOS Protein Network on Membranes. *Biophys J* **113**, 1807-1813 (2017).
47. J. K. Chung, Y. K. Lee, H. Y. Lam, J. T. Groves, Covalent Ras Dimerization on Membrane Surfaces through Photosensitized Oxidation. *J Am Chem Soc* **138**, 1800-1803 (2016).
48. G. Bollag, F. McCormick, Regulators and effectors of ras proteins. *Annu Rev Cell Biol* **7**, 601-632 (1991).
49. A. G. Stephen, D. Esposito, R. K. Bagni, F. McCormick, Dragging ras back in the ring. *Cancer Cell* **25**, 272-281 (2014).
50. S. J. Plowman, C. Muncke, R. G. Parton, J. F. Hancock, H-ras, K-ras, and inner plasma membrane raft proteins operate in nanoclusters with differential dependence on the actin cytoskeleton. *Proc Natl Acad Sci U S A* **102**, 15500-15505 (2005).
51. I. A. Prior, J. F. Hancock, Ras trafficking, localization and compartmentalized signalling. *Semin Cell Dev Biol* **23**, 145-153 (2012).
52. C. Ambrogio *et al.*, KRAS Dimerization Impacts MEK Inhibitor Sensitivity and Oncogenic Activity of Mutant KRAS. *Cell* **172**, 857-868.e815 (2018).
53. X. Nan *et al.*, Ras-GTP dimers activate the Mitogen-Activated Protein Kinase (MAPK) pathway. *Proc Natl Acad Sci U S A* **112**, 7996-8001 (2015).
54. R. Spencer-Smith *et al.*, Inhibition of RAS function through targeting an allosteric regulatory site. *Nat Chem Biol* **13**, 62-68 (2017).
55. R. Spencer-Smith *et al.*, Targeting the α4-α5 interface of RAS results in multiple levels of inhibition. *Small GTPases* **10**, 378-387 (2019).
56. M. Chen, A. Peters, T. Huang, X. Nan, Ras Dimer Formation as a New Signaling Mechanism and Potential Cancer Therapeutic Target. *Mini Rev Med Chem* **16**, 391-403 (2016).
57. S. Muratcioglu *et al.*, GTP-Dependent K-Ras Dimerization. *Structure* **23**, 1325-1335 (2015).
58. S. Muratcioglu *et al.*, Oncogenic K-Ras4B Dimerization Enhances Downstream Mitogen-activated Protein Kinase Signaling. *J Mol Biol* **432**, 1199-1215 (2020).
59. E. A. Kovrigina, A. R. Galiakhmetov, E. L. Kovrigin, The Ras G Domain Lacks the Intrinsic Propensity to Form Dimers. *Biophys J* **109**, 1000-1008 (2015).

60. J. Güldenhaupt *et al.*, N-Ras forms dimers at POPC membranes. *Biophys J* **103**, 1585-1593 (2012).
61. W. K. Gillette *et al.*, Farnesylated and methylated KRAS4b: high yield production of protein suitable for biophysical studies of prenylated protein-lipid interactions. *Sci Rep* **5**, 15916 (2015).
62. E. F. Pai *et al.*, Structure of the guanine-nucleotide-binding domain of the Ha-ras oncogene product p21 in the triphosphate conformation. *Nature* **341**, 209-214 (1989).
63. J. Rip, E. K. Van Der Ploeg, R. W. Hendriks, O. B. J. Corneth, The Role of Bruton's Tyrosine Kinase in Immune Cell Signaling and Systemic Autoimmunity. *Crit Rev Immunol* **38**, 17-62 (2018).
64. R. E. Joseph, T. E. Wales, D. B. Fulton, J. R. Engen, A. H. Andreotti, Achieving a Graded Immune Response: BTK Adopts a Range of Active/Inactive Conformations Dictated by Multiple Interdomain Contacts. *Structure* **25**, 1481-1494.e1484 (2017).
65. A. M. Scharenberg, L. A. Humphries, D. J. Rawlings, Calcium signalling and cell-fate choice in B cells. *Nat Rev Immunol* **7**, 778-789 (2007).
66. R. W. Hendriks, S. Yuvaraj, L. P. Kil, Targeting Bruton's tyrosine kinase in B cell malignancies. *Nat Rev Cancer* **14**, 219-232 (2014).
67. J. A. Márquez *et al.*, Conformation of full-length Bruton tyrosine kinase (Btk) from synchrotron X-ray solution scattering. *EMBO J* **22**, 4616-4624 (2003).
68. E. Baraldi *et al.*, Structure of the PH domain from Bruton's tyrosine kinase in complex with inositol 1,3,4,5-tetrakisphosphate. *Structure* **7**, 449-460 (1999).
69. Q. Wang *et al.*, Autoinhibition of Bruton's tyrosine kinase (Btk) and activation by soluble inositol hexakisphosphate. *Elife* **4** (2015).
70. M. Hyvönen, M. Saraste, Structure of the PH domain and Btk motif from Bruton's tyrosine kinase: molecular explanations for X-linked agammaglobulinaemia. *EMBO J* **16**, 3396-3404 (1997).
71. J. E. Ferrell, E. M. Machleder, The biochemical basis of an all-or-none cell fate switch in Xenopus oocytes. *Science* **280**, 895-898 (1998).
72. V. Papayannopoulos *et al.*, A polybasic motif allows N-WASP to act as a sensor of PIP(2) density. *Mol Cell* **17**, 181-191 (2005).
73. J. E. Johnson, J. Giorgione, A. C. Newton, The C1 and C2 domains of protein kinase C are independent membrane targeting modules, with specificity for phosphatidylserine conferred by the C1 domain. *Biochemistry* **39**, 11360-11369 (2000).

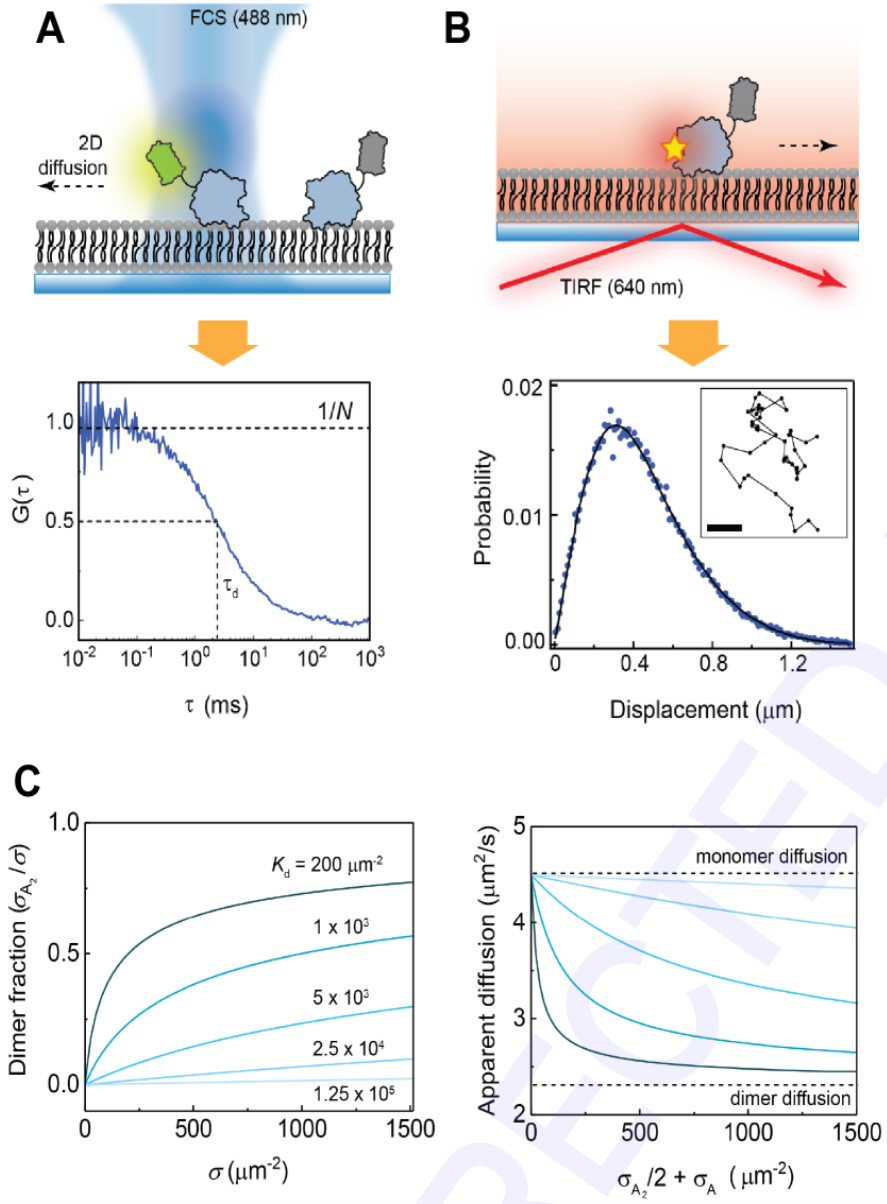

Fig. 1.

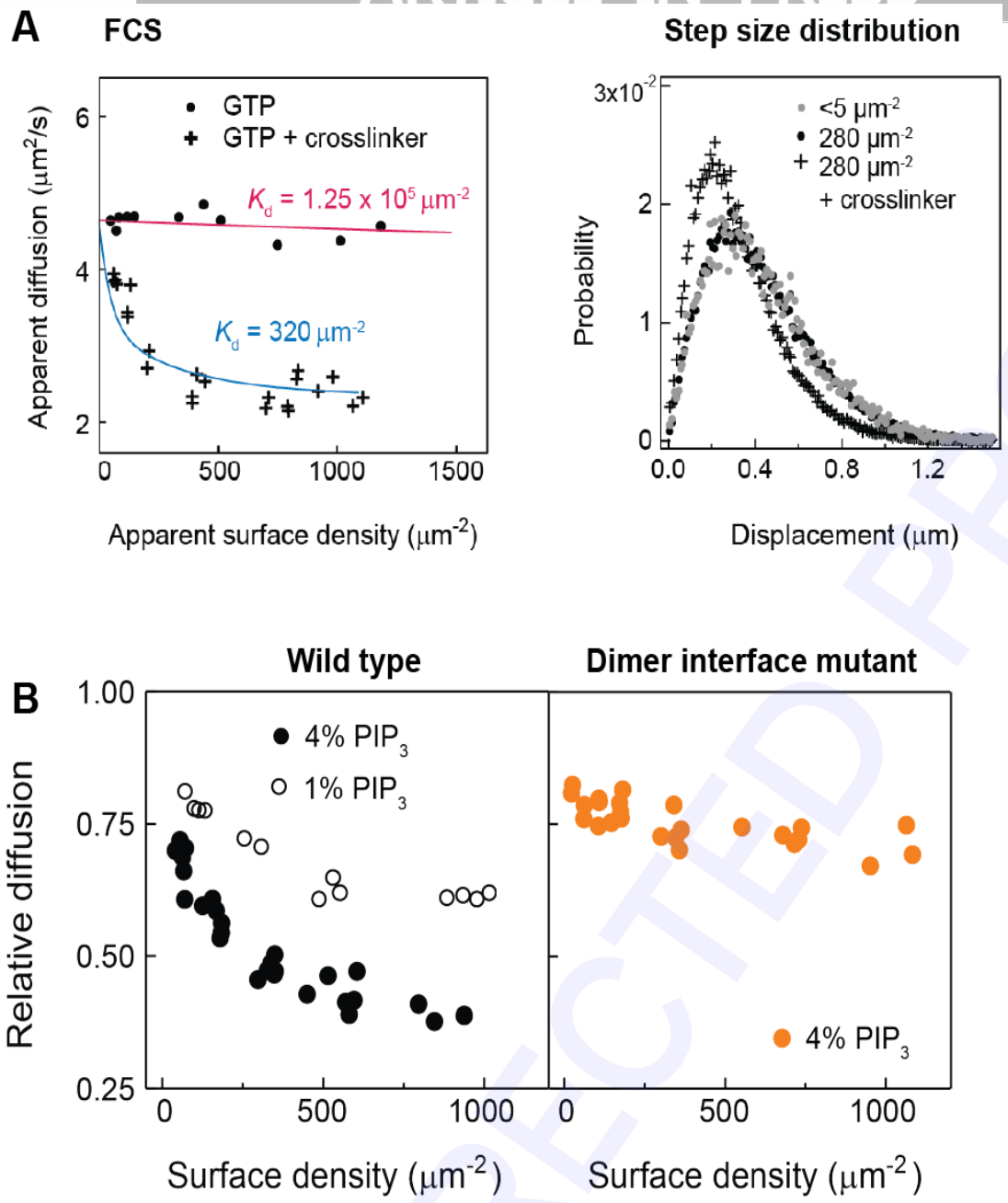

Fig. 2. Revised figure 2